

NUMERICAL STUDIES OF COSMIC RAY ACCELERATION AT COSMIC SHOCKS

HYESUNG KANG

Department of Earth Sciences, Pusan National University, Pusan 609-735, Korea

E-mail: kang@uju.es.pusan.ac.kr

(Received July 27, 2004; Accepted November 10, 2004)

ABSTRACT

Shocks are ubiquitous in astrophysical environments and cosmic-rays (CRs) are known to be accelerated at collisionless shocks via diffusive shock acceleration. It is believed that the CR pressure is important in the evolution of the interstellar medium of our galaxy and most of galactic CRs with energies up to $\sim 10^{15}$ eV are accelerated by supernova remnant shocks. In this contribution we have studied the CR acceleration at shocks through numerical simulation of 1D, quasi-parallel shocks for a wide range of shock Mach numbers and shock speeds. We show that CR modified shocks evolve to time-asymptotic states by the time injected particles are accelerated to moderately relativistic energies, and that two shocks with the same Mach number, but with different shock speeds, evolve qualitatively similarly when the results are presented in terms of a characteristic diffusion length and diffusion time. We find that $10^{-4} - 10^{-3}$ of the particles passed through the shock are accelerated to form the CR population, and the injection rate is higher for shocks with higher Mach number. The time asymptotic value for the CR acceleration efficiency is controlled mainly by shock Mach number, and high Mach number shocks all evolve towards efficiencies $\sim 50\%$, regardless of the injection rate and upstream CR pressure. We conclude that the injection rates in strong quasi-parallel shocks are sufficient to lead to significant nonlinear modifications to the shock structures, implying the importance of the CR acceleration at astrophysical shocks.

Key words : acceleration of particles – cosmology – cosmic rays – hydrodynamics – methods:numerical

I. INTRODUCTION

Cosmic rays constitute an important component of the interstellar medium (ISM) of our Galaxy, since their energy density is comparable to that of gas thermal energy or magnetic field in the Galactic disk (Blandford & Eichler 1987). The presence of galactic CR electrons is often illuminated by the radio synchrotron emission, while that of CR protons is revealed mainly by gamma ray emission from the decay of neutral pions generated from collisions between CR protons and the ISM (i.e. $p + p \rightarrow \pi^0 \rightarrow \gamma$ ray) (Longair 1992).

Supernovae (SNe) are the most energetic phenomena occurring in our Galaxy and their energy feedback to the ISM plays important roles in the evolution of our Galaxy. Assuming that on average one SN explodes every 30 years and about 10 % of the explosion energy (10^{51} erg) is deposited to CRs, they are only viable candidates to explain the CR luminosity of our Galaxy, $L_{CR} = 10^{41}$ erg s $^{-1}$ (Blandford & Eichler 1987). Numerical studies have shown that order of 10 % of SN explosion energy can be transferred into cosmic rays via diffusive shock acceleration (DSA), although the exact fraction depends on the detailed model parameters (e.g., Berezhko *et al.* 1995; Berezhko & Völck 2000). According to the standard acceleration model

where we assume a spherically symmetric shock propagating into the uniform ISM with a mean magnetic field parallel to the shock normal, the maximum energy of the particles that can be accelerated by a typical SNR is about 10^{14} eV for protons (Lagage & Cesarsky 1983). Support for rapid and efficient CR acceleration at supernova remnants (SNRs) has been provided by recent X-ray observations of young SNRs such as SN1006 and Cas A that indicate the presence of short-lived, TeV electrons emitting nonthermal synchrotron emission immediately inside the outer SNR shock (Koyama *et al.* 1995; Bamba *et al.* 2003). However, a source of nucleonic galactic CRs has not been firmly identified yet, despite the claim of detection of γ rays from RX J1713.7-3946 (Butt *et al.* 2003). On the other hand, CR electrons are also indicated by extended, diffuse nonthermal emissions in some galaxy clusters: i.e., radio synchrotron emission (Giovannini & Feretti 2000), inverse Compton scattering of cosmic background radiation in hard X-ray (Fusco-Femiano *et al.* 1999) and EUV (Lieu *et al.* 1996).

Collisionless shocks form ubiquitously in astrophysical environments via collective electromagnetic viscosities, when supersonic disturbances propagate into tenuous, magnetized, cosmic plasmas. For quasi-parallel shocks, in which the ambient magnetic field is aligned with the shock normal, the applicability of DSA theory is now fairly well established. Due to incomplete

plasma thermalization at collisionless shocks, some suprathermal particles leak upstream and their streaming motions against the background fluid generate strong MHD Alfvén waves upstream of the shock (e.g., Wentzel 1974; Bell 1978; Lucek & Bell 2000). Although these self-excited MHD waves provide necessary electromagnetic viscosities to confine thermal particles to the downstream region of the shock, some suprathermal particles in the high energy tail of the Maxwellian velocity distribution may re-cross the shock upstream. Then these particles are scattered back downstream by those same waves and can be accelerated further to higher energies via Fermi first order process (Drury 1983). Hence cosmic ray particles are natural byproducts of the collisionless shock formation process, and they are extracted from the shock-heated thermal particle distribution (Malkov & Völk 1998, Malkov & Drury 2001). Here we refer to cosmic rays as nonthermal particles above the Maxwellian distribution in momentum space, so they include nonrelativistic, suprathermal particles as well as relativistic particles. According to the DSA theory, as much as $10^{-4} - 10^{-3}$ of the particle flux passing through the shock can be injected into the CR population, the CR pressure would dominate and the nonlinear feedback to the underlying flow would become substantial. (e.g., Berezhko *et al.* 1995; Kang, Jones & Giesler 2002; Kang & Jones 2002; Kang 2003).

In the next section we briefly describe our numerical simulations. The simulation results are presented and discussed in §III, followed by a summary in §IV.

II. NUMERICAL METHODS

(a) Basic Equations

We solve the standard gasdynamic equations with CR pressure terms added in the conservative, Eulerian formulation for one dimensional plane-parallel geometry:

$$\frac{\partial \rho}{\partial t} + \frac{\partial(\rho u)}{\partial x} = 0, \quad (1)$$

$$\frac{\partial(\rho u)}{\partial t} + \frac{\partial(\rho u^2 + P_g + P_c)}{\partial x} = 0, \quad (2)$$

$$\frac{\partial(\rho e_g)}{\partial t} + \frac{\partial(\rho e_g u + P_g u + P_c u)}{\partial x} = -L(x, t), \quad (3)$$

where P_g and P_c are the gas and the CR pressure, respectively, $e_g = P_g/[\rho(\gamma_g - 1)] + u^2/2$ is the total energy density of the gas per unit mass and the rest of the variables have their usual meanings. The injection energy loss term, $L(x, t)$, accounts for the energy of the suprathermal particles injected to the CR component at the subshock (see Kang *et al.* 2002 for details). The term $L(x, t)\Delta t$ is subtracted from the gas thermal energy in the immediate postshock region in order to conserve the total energy.

The diffusion-convection equation for the pitch angle averaged CR distribution function, $f(p, x, t)$, (e.g., Skilling 1975) is given by

$$\frac{\partial f}{\partial t} + u \frac{\partial f}{\partial x} = \frac{1}{3} \left(\frac{\partial u}{\partial x} \right) p \frac{\partial f}{\partial p} + \frac{\partial}{\partial x} (\kappa(x, p) \frac{\partial f}{\partial x}). \quad (4)$$

and $\kappa(x, p)$ is the spatial diffusion coefficient. For convenience we always express the particle momentum, p in units $m_p c$. Then the CR pressure is calculated from the nonthermal particle distribution as follows:

$$P_c = \frac{4}{3} \pi m_p c^2 \int_0^\infty \frac{f(p) p^4 dp}{\sqrt{p^2 + 1}}. \quad (5)$$

(b) CRASH: CR/AMR Hydrodynamics Code

Unlike ordinary gas shocks, the CR shock includes a wide range of length scales associated not only with the dissipation into “thermal plasma”, but also with the nonthermal particle diffusion process. Those are characterized by the so-called diffusion lengths,

$$x_d(p) = \kappa(p)/u_s, \quad (6)$$

where $\kappa(p)$ is the spatial diffusion coefficient for CRs of momentum p , and u_s is the characteristic flow velocity (Kang & Jones 1991). Accurate solutions to the CR diffusion-convection equation require a computational grid spacing significantly smaller than x_d , typically, $\Delta x \sim 0.1 x_d(p)$. On the other hand, for a realistic diffusion transport model with a steeply momentum-dependent diffusion coefficient, the highest energy, relativistic particles have diffusion lengths many orders of magnitude greater than those of the lowest energy particles.

To follow the acceleration of highly relativistic CRs from suprathermal energies, all those scales need to be resolved numerically. However, the diffusion and acceleration of the low energy particles are important only close to the shock owing to their small diffusion lengths. Thus it is necessary to resolve numerically the diffusion length of the particles only around the shock. To solve this problem generally we have developed the CRASH (Cosmic-Ray Amr SHock) code by combining a powerful “Adaptive Mesh Refinement” (AMR) technique and a “shock tracking” technique, and implemented them into a hydro/CR code based on the wave-propagation method (Kang *et al.* 2001; Kang *et al.* 2002). The AMR technique allows us to “zoom in” inside the precursor structure with a hierarchy of small, refined grid levels applied around the shock. The shock tracking technique follows hydrodynamical shocks within regular zones and maintains them as true discontinuities, thus allowing us to refine the region around the gas subshock at an arbitrarily fine level. The result is an enormous savings in both computational time and data storage over what would be required to solve the problem using more traditional methods on a single fine grid.

(c) Injection Model

In the “thermal leakage” injection model, some supra-thermal particles in the tail of the Maxwellian distribution swim successfully against the Alfvén waves advecting downstream, and then leak upstream across the subshock and get injected in the CR population. In order to model this injection process in Gieseler *et al.* (2001) we adopted a “transparency function”, $\tau_{\text{esc}}(\epsilon, v)$, which expresses the probability that supra-thermal particles at a given velocity can leak upstream through the magnetic waves, based on non-linear particle interactions with self-generated waves (Malkov and Völk 1998). The inverse wave-amplitude parameter, $\epsilon = B_0/B_\perp$, measures the ratio of the amplitude of the postshock MHD wave turbulence B_\perp to the general magnetic field aligned with the shock normal, B_0 . The breadth of the thermal velocity distribution relative the downstream flow velocity in the subshock rest-frame determines the probability of leakage, and so the injection process is sensitive to the velocity jump at the subshock, which depends on the subshock Mach number. The injection rate increases with the subshock Mach number, but becomes independent of M_s in the strong shock limit of $M_s \gtrsim 10$ (Kang *et al.* 2002). The only free parameter of the adopted transparency function is ϵ and it is rather well constrained, since $0.3 \lesssim \epsilon \lesssim 0.4$ is indicated for strong shocks (Malkov & Völk 1998).

III. SIMULATION RESULTS

We have calculated the CR acceleration at 1D quasi-parallel shocks driven by a plane-parallel piston with $u_n = 75 - 750 \text{ km s}^{-1}$ and preshock temperatures of $T_0 = 10^4 - 10^{7.6} \text{ K}$. The upstream sound speed is given by $c_{s,0} = 15 \text{ km s}^{-1} (T_0/10^4)^{1/2}$. Then the normalization constants are set by two parameters, the piston Mach number, $1.5 \leq M_0 \leq 100$, and $c_{s,0}$, through $u_n = c_{s,0} M_0$. The initial speed (u_s) of the shock driven by the piston is higher than the piston speed, u_n , and depends on the compression ratio across the shock. So Mach numbers of the resulting shocks range over $2 \leq M_s \leq 133$. Due to the nonlinear CR feedback, however, the *instantaneous* shock speed is different from the initial shock speed in CR dominated shocks.

(a) Similarity in the Dynamics of CR shocks

We assume a Bohm type diffusion model in which the diffusion coefficient is given as

$$\kappa(\rho, p) = \kappa_n \left(\frac{\rho_0}{\rho} \right) \frac{p^2}{(p^2 + 1)^{1/2}}, \quad (7)$$

where $\kappa_n = 3.13 \times 10^{22} \text{ cm}^2 \text{ s}^{-1} B_\mu^{-1}$, (B_μ is the magnetic field strength in units of microgauss) and ρ_0 is the preshock gas density far upstream. This assumption is based on the hypothesis that strong Alfvén waves are self-generated by streaming CRs and provide random

scatterings strong enough to scatter particles within one gyration radius. The assumed density dependence for κ accounts for compression of the perpendicular component of the wave magnetic field and also inhibits the acoustic instability in the precursor of highly modified CR shocks (Kang, Jones, & Ryu 1992).

In the test-particle limit where the nonlinear CR feedback is not significant, the mean acceleration time scale for a particle to reach momentum p is determined by the velocity jump at the shock and the diffusion coefficient (e.g., Drury 1983), that is,

$$\tau_{\text{acc}}(p) = \frac{3}{u_1 - u_2} \left(\frac{\kappa_1}{u_1} + \frac{\kappa_2}{u_2} \right) \approx \frac{8M_s^2}{M_s^2 - 1} t_d(p), \quad (8)$$

where the subscripts, 1 and 2, designate the upstream and downstream conditions, respectively, and $t_d(p) = \kappa(p)/u_s^2$ is the diffusion time scale and $u_s = u_1$.

The ideal gasdynamic equations in 1D planar geometry do not contain any intrinsic time and length scales, but in CR modified shocks the CR acceleration and the precursor growth can be characterized by the diffusion scales, $t_d(p)$ and $x_d(p)$. κ_n provides a useful canonical value, since nonlinear feedback from CRs to the underlying flow becomes significant typically by the time transrelativistic CRs are accelerated. Consequently, we normalize our shock evolution times and structure scales by $t_n = \kappa_n/u_n^2$, and $x_n = \kappa_n/u_n$, respectively. *One expects intrinsic similarities in the dynamic evolution and structure of two CR shock models with the same Mach number, but with different shock speeds, so long as the results are expressed in terms of t_n and x_n .*

(b) Characteristics of 1D Plane-parallel CR Shocks

Once shocks develop nonlinear properties in response to CR feedback, there are several important characteristics that distinguish them from more familiar gasdynamic shocks: 1) CR shocks continue to evolve over relatively long times and broaden as they do so. While full thermalization takes place instantaneously at a simple, discontinuous jump in an “ideal” gasdynamic shock, CR acceleration and the corresponding modifications to the underlying flow depend on supra-thermal particles passing back and forth diffusively across the shock structure. These processes develop, therefore, on the diffusion time scale, t_d , and diffusion length scale, x_d . Generally, these scales are expected to be increasing functions of particle momentum, so CR acceleration and shock evolution rates slow over time. 2) CR diffusion upstream of the shock discontinuity leads to strong pressure gradients in a shock precursor, enhancing the total compression through the shock transition over that in the “viscous” subshock. The total compression through a high-Mach-number CR shock can greatly exceed the canonical value $r = (\gamma_g + 1)/(\gamma_g - 1)$ for strong gasdynamical shocks (where γ_g is the gas adiabatic index). 3) Both the effective compressibility of the combined thermal-CR plasmas and the mean CR diffusion

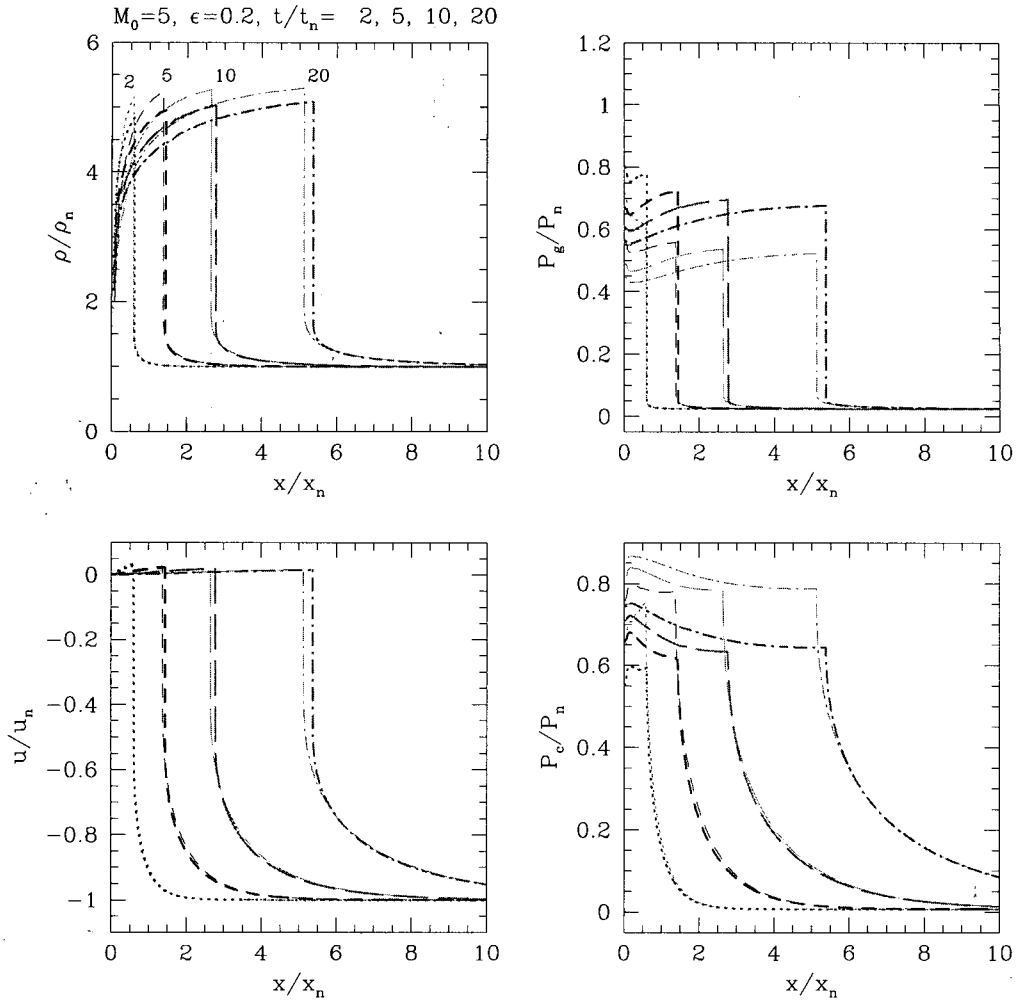


Fig. 1.— Time evolution of the shocks driven by 1D accretion flows with $M_0 = u_n/c_{s,0} = 5$ is shown at normalized times, $t/t_n = 2, 5, 10,$ and 20 . The accretion flows are reflected at $x/x_n = 0$ and shocks with $M_s = 6.8$ propagate to the right. The leftmost profile corresponds to the earliest time. Light lines represent a flow with $u_n = 75 \text{ km s}^{-1}$, $T_0 = 10^4 \text{ K}$, and a pre-existing CR population with $f_{up} \propto (p/p_M)^{-4.7}$. Heavy lines represent the model with $u_n = 750 \text{ km s}^{-1}$, $T_0 = 10^6 \text{ K}$, and $f_{up} \propto (p/p_M)^{-4.5}$. For both models the pre-existing upstream CR pressure is $P_{c,0}/P_{g,0} = 0.25$. The normalization diffusion time scale, $t_n = \kappa_n/u_n^2$, and diffusion length, $x_n = \kappa_n/u_n$ are defined by the accretion speed of each model. The inverse wave-amplitude parameter $\epsilon = 0.2$ is adopted for both models.

coefficient increase over time as relativistic CRs absorb more energy and as escaping CRs remove energy from the shock structure. Details of these properties depend on the CR momentum distribution. Thus, downstream states of the CR modified shock cannot be found from simple “shock jump conditions”, but rather have to be integrated time-dependently from given initial states or, for steady solutions, found in terms of some predefined limits to the CR spectrum (*e.g.*, an upper momentum cutoff). 4) Energy transfer to the CRs rather than to the thermalized gas in the shock transition reduces the downstream thermal energy of a CR modified shock compared to a gasdynamic shock with the same shock speed and Mach number.

Figure 1 illustrates these characteristics very well. Three key stages of shock evolution in response to CR

feed back can be defined: 1) Development of the shock precursor that slows and heats the flow entering the gas subshock, reducing the Mach number of the latter; 2) achievement of an *approximately* time-asymptotic dynamical shock transition, including nearly steady post-shock CR and gas pressures; 3) continued, approximately “self-similar” evolution of the shock structure for Bohm-type diffusion, as CRs are accelerated to ever higher momenta. Once stage (3) is reached, there is little change in the dynamical properties of the shocks, and, in particular, little change in the total efficiency with which kinetic energy is transferred to CRs.

Time evolution of the distribution function $g(p) = f(p)p^4$ at the gas subshock is shown in figure 2 for the models with $T_0 = 10^6 \text{ K}$ and with $f_{up} \propto p^{-4.5}$. The dotted line shows the initial Maxwellian distribution

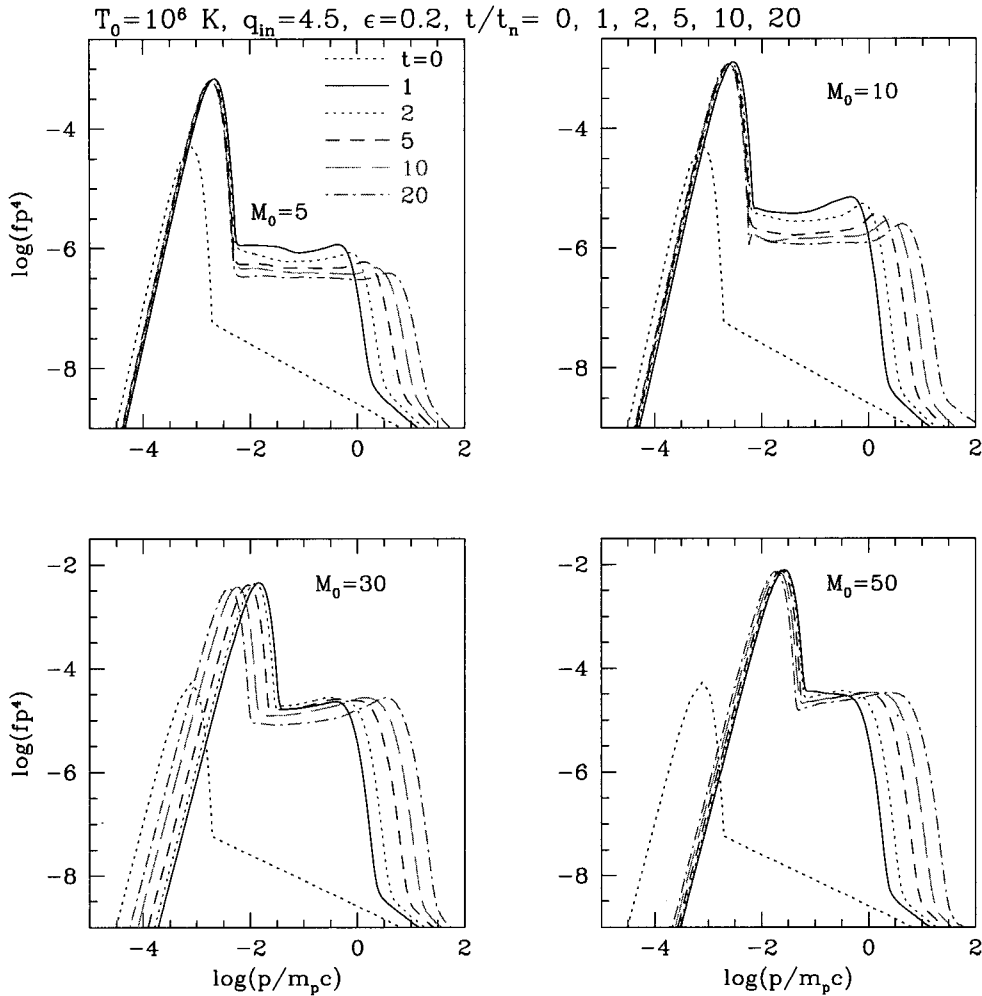


Fig. 2.— Evolution of the CR distribution function at the shock, represented as $g = p^4 f(p)$, is plotted for the models of $M_0 = 5, 10, 30$, and 50 with $T_0 = 10^6$ K and $f_{up} \propto (p/p_M)^{-4.5}$. The CR spectrum of the preshock flow is represented by the dotted line. For all models shown here the pre-existing upstream CR pressure is $P_{c,0}/P_{g,0} = 0.25$.

with T_0 and the specified power-law distribution for the pre-existing CR population. The postshock thermal distribution during the early evolution (before shock modification) should have $T_2 \propto M_0^2$, so the injection momentum, $p_{inj} \propto M_0$ for $t/t_n < 1$. However, as energy transfer to CRs increases over time and the gas subshock weakens, the peak in the Maxwellian distribution shifts to lower momenta. The model with $M_0 = 30$ shows this effect clearly. This nonlinear feedback is greater for higher Mach number, so that the postshock temperature of evolved CR modified shocks depends on M_0 much more weakly than the standard M_0^2 . We note that the Maxwellian distribution is calculated from the gas temperature and density, while the CR distribution is calculated by the diffusion-convection equation given in equation (4). The distribution function shows the characteristic “concave upwards” curves reflecting modified shock structure (including the precursor) for the models with $M_0 = 10$ and 30 .

(c) Injection and Acceleration Efficiencies

We define the injection efficiency as the fraction of particles that have entered the shock from far upstream and then are injected into the CR distribution:

$$\xi(t) = \frac{\int_0^{x_{max}} dx \int_{p_0}^{p_1} 4\pi f(p, x, t) p^2 dp}{\int_{t_1}^t n_0 u'_s(t') dt'} \quad (9)$$

where n_0 is the particle number density far upstream, u'_s is the instantaneous shock speed, and t_1 is the time when the CR injection/acceleration is turned on.

Figure 3 illustrates the time averaged injection efficiency, $\xi(t)$, for models without pre-existing CRs. The calculated injection efficiency ranges from \sim a few $\times 10^{-5}$ to $\sim 10^{-3}$, depending on the subshock Mach number, the shock speed, and the injection parameter, ϵ . The modeled thermal-leakage injection process is less efficient for weaker subshocks and for smaller ϵ (stronger wave trapping of suprathermal particles in

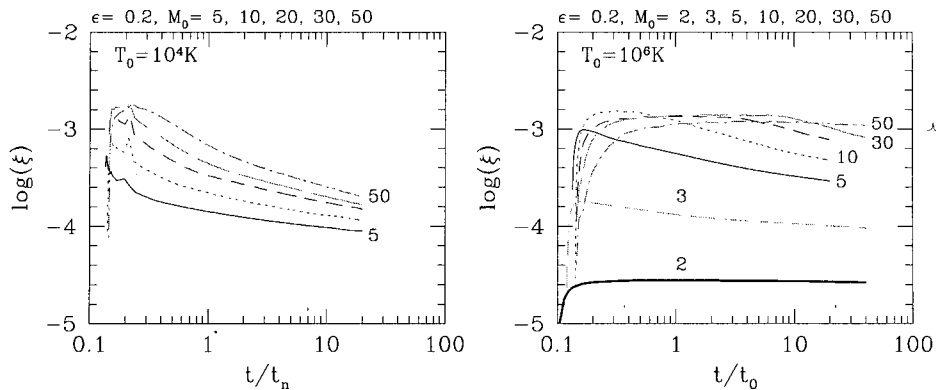


Fig. 3.— Time averaged injection efficiency, $\xi(t)$, for models without pre-existing CRs. Left panel shows the models with $M_0 = 5 - 50$ and $T_0 = 10^4$ K, while right panel shows the models with $M_0 = 2 - 50$ and $T_0 = 10^6$ K.

the postshock environment). Injection is also less efficient for lower shock speeds, because the diffusive flux of injected particles crossing the subshock is smaller for smaller injection momentum ($p_{inj} \propto u_s$). So, for a given Mach number the models with higher shock speed (*i.e.*, higher T_0 in figure 3) have larger values of $\xi(t)$. For strong shocks the subshock weakens significantly due to the CR nonlinear feedback, so the injection efficiency slowly decreases over time.

As a measure of acceleration efficiency, we define the “CR energy ratio”; namely the ratio of the total CR energy within the simulation box to the kinetic energy in the *initial shock frame* that has entered the simulation box from far upstream,

$$\Phi(t) = \frac{\int_0^{x_{max}} dx E_{CR}(x, t)}{0.5 \rho_0 (u'_{s,0})^3 t}, \quad (10)$$

where $u'_{s,0}$ is the initial shock speed.

Figure 4 shows the CR energy ratio, Φ , for models with different M_0 , $P_{c,0}$, and T_0 . The injection parameter is the same for all models, $\epsilon = 0.2$. We find that time asymptotic values of Φ increase with M_0 but approach ~ 0.5 for $M_0 > 20$, and that Φ increases with the presence of upstream CRs for models with $M_0 < 5$. Comparison of models with the same M_0 but with different T_0 (*i.e.*, different u_s) tells us that the CR acceleration is slower to develop (in terms of t/t_n) and the time asymptotic CR acceleration efficiency is slightly lower for the models with higher T_0 ,

IV. SUMMARY

Unlike pure gasdynamic shocks, downstream states of the CR modified shocks cannot be found from “shock jump conditions”, so they have to be integrated time-dependently from given initial states or found from nonlinear analytical methods. We have performed such time-dependent simulations in order to study the CR acceleration at quasi-parallel astrophysical shocks.

The main results of our simulations can be summarized as follows:

1) The CR pressure approaches a steady-state value in a time scale comparable to the acceleration time scales for mildly relativistic protons after which the evolution of CR modified shocks becomes approximately “self-similar”.

2) Two shocks with the same Mach number, but with different shock speeds, evolve qualitatively similarly when the results are presented in terms of a characteristic diffusion length and diffusion time. So the acceleration efficiency is determined mostly by the shock Mach number. Such similarities are only approximate, however, because the partial CR pressure and the Bohm diffusion coefficient for transrelativistic CRs do depend on the momentum $m_p c$. Since the effective injection momentum is $p_{inj}/m_p c \propto (u_s/c)$, the initial evolution depends on the shock speed as well as Mach number.

3) Suprathermal particles can be injected very efficiently into the CR population via the thermal leakage process, so that typically a fraction of $10^{-4} - 10^{-3}$ of the particles passed through the shock become CRs for $\epsilon = 0.2 - 0.3$.

4) For a given value of ϵ , the acceleration efficiency increases with the shock Mach number, but approaches a similar value in the strong shock limit. Time asymptotic values of the ratio of CR energy to inflowing kinetic energy converge to $\Phi \approx 0.5$ for $M_s \gtrsim 30$ and it is relatively independent of other upstream or injection parameters. Thus, strong quasi-parallel shocks can be mediated mostly by CRs and the gas thermal energy can be up to ~ 10 times smaller than that expected for gasdynamic shocks.

5) For weak shocks, on the other hand, the acceleration efficiency increases with the injection rate (or ϵ) and the pre-existing CRs. The presence of a pre-existing CR population acts effectively as a higher injection rate than the thermal leakage alone, leading to greatly enhanced CR acceleration efficiency in low Mach number

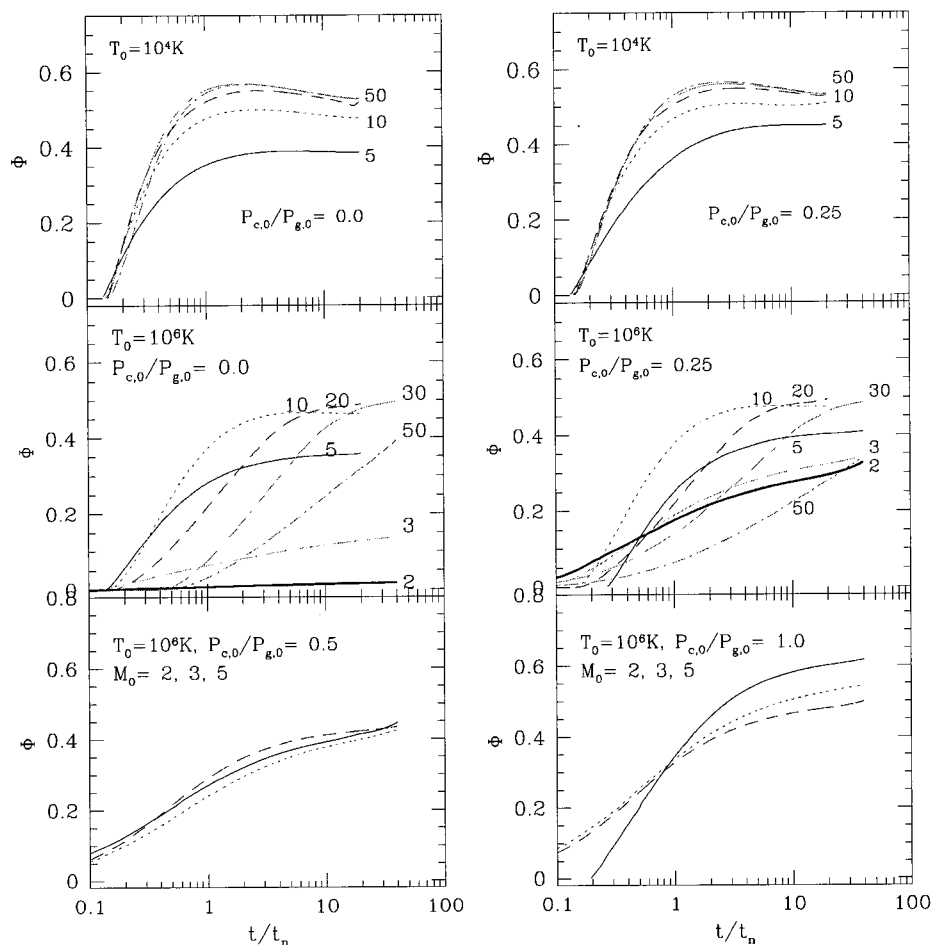


Fig. 4.— Time evolution of the ratio of total CR energy in the simulation box to the kinetic energy in the initial shock rest frame that has entered the simulation box from upstream, $\Phi(t)$. Top panels show the models with $M_0 = 5 - 50$, $T_0 = 10^4$ K, while middle panels show the models with $M_0 = 2 - 50$, $T_0 = 10^6$ K. For the top and middle panels, the left panels are for the models without pre-existing upstream CRs, while the right panels are for the models with $P_{c,0} = 0.25P_{g,0}$. Bottom panels show the low Mach number models with $M_0 = 2 - 5$, $T_0 = 10^6$ K and different levels of upstream CRs.

shocks. We found, even for weak shocks of $M_s = 3$, that up to 40 % of the total energy flux through the shocks can be transferred to CRs, when the upstream CR pressure is comparable to the gas pressure in the preshock flow.

ACKNOWLEDGEMENTS

This work was supported by KOSEF through Astrophysical Research Center for the Structure and Evolution of Cosmos (ARCSEC) and grant-R01-1999-00023 and by Pusan National University Research Grant.

REFERENCES

- Bamba, A., Yamazaki, R., Ueno, M. & Koyama, K. 2003, *ApJ*, 589, 827
- Bell, A.R. 1978, *MNRAS*, 182, 147
- Berezhko, E., Ksenofontov, L., & Yelshin, V. 1995, *Nuclear Phys B.*, 39, 171.
- Berezhko E.G., and Völk H.J. 2000, *A&Ap*, 357, 283
- Blandford, R. D., & Eichler, D. 1987, *Phys. Rept.*, 154, 1
- Butt, Y. M., Torres, D. F., Romero, G. E., Dame, T. M., Combi, J. A, 2002, *Nature*, 418, 499
- Drury, L. O’C. 1983, *Rept. Prog. Phys.*, 46, 973
- Fusco-Femiano, R., Dal Fiume, D., Feretti, L., Giovannini, G., Grandi, P., Matt, G., Molendi, S. & Santangelo, A. 1999, *ApJ*, 513, L21
- Gieseler U.D.J., Jones T.W., & Kang H. 2000, *A&Ap*, 364, 911
- Giovannini, G. & Feretti, L. 2000, *New Astronomy*, 5, 335
- Kang, H., 2003, *Journal of Korean Astronomical Society*, 36, 1
- Kang, H., & Jones, T. W. 1991, *MNRAS*, 249, 439
- Kang, H., & Jones, T. W., 2002, *Journal of Korean Astronomical Society*, 35, 159
- Kang, H., Jones, T. W., Ryu, D. 1992, *ApJ*, 385, 193

- Kang, H., Jones, T. W., & Gieseler, U.D.J, 2002, ApJ, 579, 337
- Kang, H., Jones, T. W., LeVeque, R. J., & Shyue, K. M. 2001, ApJ, 550, 737
- Koyama, K. , Petre, R., Gotthelf, E. V. et al. 1995, Nature, 378, 255
- Lagage, P.O., & Cesarsky, C.J. 1983, A&Ap, 118, 223
- Lieu, R., Mittaz, J. P. D., Bowyer, S., Lockman, F. J., Hwang, C.-Y. & Schmitt, J. H. M. M. 1996, ApJ, 458, L5
- Longair, M. S., 1992, in High Energy Astrophysics (the University Press: Cambridge)
- Lucek, S.G., & Bell, A.R. 2000, MNRAS, 314, 65
- Malkov M.A., & Drury, L.O'C. 2001, Rep. Progr. Phys. 64, 429
- Malkov, M.A., & Völk H.J. 1998, Adv. Space Res. 21, 551
- Skilling J. 1975, MNRAS, 172, 557
- Wentzel, D. G., 1974, ARAA, 12, 71